https://doi.org/10.15407/ujpe70.3.151

O.M. GORBACHENKO, V.A. PLUJKO

Taras Shevchenko National University of Kyiv
*(60, Volodymyrs'ka Str., Kyiv 01033, Ukraine; e-mail: plujko@gmail.com)*

# DEFORMATION PARAMETERS OF ATOMIC NUCLEI FROM PHOTOABSORPTION DATA AND THEIR IMPACT ON PHOTOABSORPTION CROSS-SECTION

*The values of the effective quadrupole deformation parameter of atomic nuclei have been calculated, and their uncertainties have been estimated. The approximation of axially symmetric nuclei and the energy splitting values of two modes of the isovector giant dipole resonance (GDR) for the photoabsorption cross-sections of 144 isotopes from $^{6}Li$ to $^{239}Pu$ are used. For axially symmetric atomic nuclei with $155 < A < 190$ and $225 < A < 250$, the determined effective values of the quadrupole deformation parameter are exactly identical to the values of the quadrupole deformation parameter $\beta$. The results are compared with the values obtained in other approaches. It is demonstrated that the obtained absolute values of the quadrupole deformation parameter for the GDR excitation, as a rule, coincide, within the uncertainty limits, with the absolute values of deformations in the ground nucleus state. For the $^{100}Mo$ and $^{178}Hf$ nuclei, the dependences of the partial photoabsorption cross-sections on the GDR characteristics are calculated and analyzed.*

*K e y w o r d s*: photoabsorption cross-sections, axially deformed nuclei, nucleus quadrupole deformation parameters, isovector giant dipole resonance, energy splitting.

## 1. Introduction

Surface deformation is one of the most important macroscopic characteristics of atomic nuclei, which helps one to understand their spatial structure. The values of the deformation parameter are necessary for the calculation of observable quantities in various nuclear processes in the framework of macroscopic models. Experimental and theoretical studies [1, 2] have shown that deformed nuclei with the atomic numbers $A$ in the rare-earth ($155 < A < 190$) and actinide ($225 < A < 250$) intervals have the shape of ellipsoids in the ground state. In such axially symmetric nuclei, the nucleus radius is determined by the expression

$$R(\theta) = R'_0(\beta)(1 + \beta Y_{20}(\theta, \varphi)) \equiv R'_0(\alpha)(1 + \alpha P_2(\theta)),$$

where $Y_{20}(\theta, \varphi)$ and $P_2(\theta)$ are spherical harmonics and second-order Legendre polynomials, respectively; $\theta$ is the polar angle in the inner system with the ordinate axis directed along the nucleus symmetry axis; $R'_0$ is a parameter characterizing the conservation of the nucleus volume; $R'_0(\beta = 0) = R_0$ is the radius of a spherical nucleus with the equivalent volume, but with the uniform distribution; and $R_0 = r_0 A^{1/3}$, $\beta$, and $\alpha = (5/4\pi)^{1/2}\beta \approx 0.631\beta$ are quadrupole deformation parameters.

There are various tables for the values of quadrupole deformation parameters obtained from experimental data. For example, the signs and the absolute values of the quadrupole deformation parameter $\beta$ can be calculated using experimental data for the internal electric quadrupole moment $Q_0 \approx \approx ZR_0^2\beta + O(\beta^2)$, where $Z$ is the nuclear charge [3–5].

In work [6], experimental data on the scattering of alpha particles with medium energies (20–140 MeV) were used to find the $\beta$-parameter values. The data were analyzed using the methods of coupled channels and Blair phase shift. The experimental data on the probabilities of *E2* gamma transitions between the ground state and the first excited rotational state

C i t a t i o n: Gorbachenko O.M., Plujko V.A. Deformation parameters of atomic nuclei from photoabsorption data and its impact on photoabsorption cross sections. *Ukr. J. Phys.* **70**, No. 3, 151 (2025). https://doi.org/10.15407/ujpe70.3.151.
© Publisher PH "Akademperiodyka" of the NAS of Ukraine, 2025. This is an open access article under the CC BY-NC-ND license (https://creativecommons.org/licenses/by-nc-nd/4.0/)

$2^+$ are proportional to the square of the internal quadrupole moment. Therefore, they make it possible to calculate the absolute values of the $\beta$ parameter for even-even nuclei [7–9].

In the photoabsorption cross-sections of axially symmetric nuclei, two resonance peaks are observed [10–21]. The difference between their energies (the energy splitting of the isovector giant resonance) determines the value of the quadrupole deformation parameter $\beta$. For axially symmetric deformed nuclei, this circumstance was first demonstrated in the works by Danos [22] and Okamoto [23]. In the work by Danos [22], the calculations were performed in the framework of a generalized Steinwedel–Jensen hydrodynamic model. Further studies have shown that this hydrodynamic model can be reliably applied for medium and heavy atomic nuclei [10, 24–29].

In this work, the values of the quadrupole deformation parameter were obtained from the GDR energy splitting in the photoabsorption cross-sections of deformed nuclei, and their uncertainties were estimated.

The values of the GDR mode energies and contributions were taken from the tables in works [19, 21]. The results were compared with the values obtained in other approaches [6, 8, 9], as well as with the database in the file "deflib.dat" [30], where they were calculated using the macro-microscopic approach [31].

For the $^{100}$Mo and $^{178}$Hf nuclei, the photoabsorption cross-sections calculated using various values of the GDR characteristics were compared.

## 2. Determination of the Quadrupole Nucleus Deformation Parameters and Their Comparison with Other Data

According to the generalized hydrodynamic model of Danos [22, 24], the following relationship holds between the energies of two $E_a$ and $E_b$ modes of GDR excitation:

$$\frac{E_b}{E_a} = c_0 + c_1 \frac{R_a}{R_b} \quad (c_0 = 0.089,\ c_1 = 0.911), \tag{1}$$

where the quantities $R_a = R(\theta = 0) = R'_0(\alpha)(1+\alpha)$ and $R_b = R(\theta = \pi/2) = R'_0(\alpha)(1-\alpha/2)$ are the semiaxes directed along and perpendicular to the nucleus symmetry axis, respectively; and $E_a$ and $E_b$ are the energies of the corresponding vibrational modes. Formula (1) can be rewritten in the form

$$\frac{R'_0 - R_b}{R'_0} = \frac{\frac{E_b}{E_a} - c_0 - c_1}{\frac{E_b}{E_a} - c_0 + 2c_1} = \frac{\frac{E_b}{E_a} - 1}{\frac{E_b}{E_a} + 1.733}, \tag{2}$$

whence

$$\beta = \sqrt{\frac{4\pi}{5}} \frac{2(E_b - E_a)}{E_b + (c_0 + 2c_1)E_a} = \\ = 3.17 \frac{E_b - E_a}{E_b + 1.733 E_a}. \tag{3}$$

Since the $\beta$-dependence of the energy difference between the GDR modes begins with a linear component, the approximation

$$E_b + 1.733 E_a = 2.733(E_a + E_b)/2 + O(\beta)$$

can be used in the denominator of this formula in the linear approximation in deformation. Then expression (3) takes the form

$$\beta \approx \sqrt{\frac{4\pi}{5}} \frac{4}{2.733} \frac{E_b - E_a}{E_a + E_b} = 2.32 \frac{E_b - E_a}{E_a + E_b}. \tag{4}$$

One can see that the absolute value of the deformation parameter $\beta$ is determined by the absolute value of the difference between the energies of the GDR excitation modes, and its sign depends on the ratio between them. If $E_a > E_b$, then the nucleus has the shape of a prolate ellipsoid of rotation ($\beta > 0$), and if $E_a < E_b$, the nucleus is an oblate ellipsoid of rotation ($\beta < 0$).

Which of the two resonance energies corresponds to the energy of oscillations along the nucleus symmetry axis and which is perpendicular to it can be determined on the basis of the contributions made by the resonances to the integrated photoabsorption cross-section. One normal oscillation mode of the isovector nucleon density is excited along the symmetry axis, and two modes in the plane perpendicular to the symmetry axis. Therefore, for the photoabsorption of unpolarized photons, it is expectable that the excitation probabilities of each oscillation mode are close to one another so that the following relationship holds for the contributions of the modes to the integrated photoabsorption cross-section:

$$s_b > s_a. \tag{5}$$

Then, provided the same excitation probability for each vibration mode, we obtain [10, 22, 24]

$$s_b = 2s_a, \quad s_a + s_b = 2s_\Sigma, \tag{6}$$

where $s_\Sigma = 1.0$.

Thus, if we denote the energies of two resonance peaks as $E_1$ and $E_2$ ($E_2 > E_1$) and the contributions of the corresponding resonances to the integrated cross-section as $s_1$ and $s_2$, then, for $s_2 > s_1$, we have $E_1 = E_a$ and $E_2 = E_b$, and the nucleus is prolate ($\beta > 0$), whereas, for $s_1 > s_2$, we have $E_1 = E_b$ and $E_2 = E_a$, and the nucleus is oblate ($\beta < 0$).

Note that, unlike formula (3), relationship (4) allows the calculation of the absolute value of the quadrupole nucleus deformation parameter without analyzing the relation among the photopeak energies and the energies of the vibration modes along and perpendicular to the nucleus symmetry axis,

$$|\beta| \approx 2.32\,\frac{E_2 - E_1}{E_1 + E_2}. \tag{7}$$

We applied relationships (1)–(7) while calculating the quadrupole deformation parameter. The values for the energies and contributions of the GDR modes were taken from tables in works [19, 21], where they were obtained by fitting the photoabsorption cross-sections in the axially-symmetric-nucleus approximation.

We also calculated the root-mean-square uncertainties of the deformation parameter, $\sigma_\beta$, from the uncertainties of the GDR mode energies, $\sigma_{E_{a,b}}$, using the error-transfer method [32],

$$\sigma_\beta = \sqrt{\left(\frac{\partial\beta}{\partial E_a}\sigma_{E_a}\right)^2 + \left(\frac{\partial\beta}{\partial E_b}\sigma_{E_b}\right)^2}, \tag{8}$$

where, according to Eqs. (3) and (4), the general forms of the derivatives look like

$$\begin{aligned}\frac{\partial\beta}{\partial E_a} &= a_a\frac{E_b}{(E_b + b_a E_a)^2},\\ \frac{\partial\beta}{\partial E_b} &= a_b\frac{E_b}{(E_b + b_b E_a)^2}.\end{aligned} \tag{9}$$

For the exact relationship (3), the values of the coefficients $a_{a,b}$ and $b_{a,b}$ are $a_a = -a_b = -8.66$ and $b_a = b_b = 1.733$, and for the approximate expression (4), $a_a = -a_b = -4.64$ and $b_a = b_b = 1.0$. The root-mean-square errors for the GDR excitation mode energies were taken from the tables in work [19].

Note that the GDR characteristics were found after subtracting the quasideuteron contribution [33] obtained from fitting the experimental values of the photoabsorption cross-sections by expressions of the standard and modified Lorentzians (hereafter, the SLO and SMLO approaches, respectively) [14, 17, 20, 34–36, 38]. The experimental values of the total photoabsorption cross-sections were obtained either from the EXFOR database [37] or by combining experimental partial cross-sections that were the most suitable for approximating the total photoabsorption cross-section. The GDR parameters were obtained [19] for 144 isotopes from $^6$Li to $^{239}$Pu atomic nuclei. In the rare-earth ($155 < A < 190$) and actinide ($225 < A < 250$) intervals, the atomic nuclei are axially symmetric in the ground state, and the obtained $\beta$-values are the values of the quadrupole shape deformation parameter, whereas, for other nuclei, $\beta \equiv \beta_{\text{eff}}$ is the effective parameter of nucleus deformation if the nucleus shape is approximated by an ellipsoid of rotation.

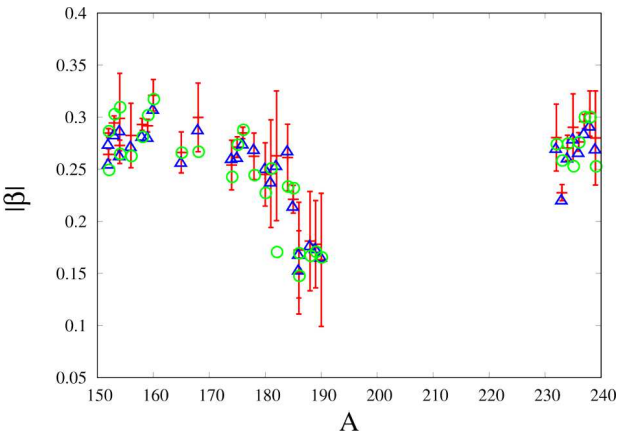


***Fig. 1.*** Absolute values of the deformation parameter in axially symmetric nuclei calculated by formulas (3) and (7) with GDR energies in the SLO and SMLO approaches. Symbols: crosses with error bars – SLO model (Eq. (3)), triangles – SLO model (Eq. (7)), circles – SMLO model (Eq. (3))

In Fig. 1, the absolute values of the deformation parameter are illustrated which were calculated by formulas (3) and (7) with the GDR energies determined in the framework of the SLO and SMLO models (Eq. (3)) for axially symmetric nuclei. The deformation parameter values obtained in the SLO model (Eq. (3)) are supplied with error bars obtained using formulas (8) and (9), and the parameter values for the SLO model were calculated according to formula (7). The values of the parameter $\beta$ calculated in the SMLO approach according to formula (3) are presented without error bars. Hereafter, for clarity, the isobar values are spaced by $\pm 0.1$ along the abscissa axis. One can see from the figure that the $|\beta|$-

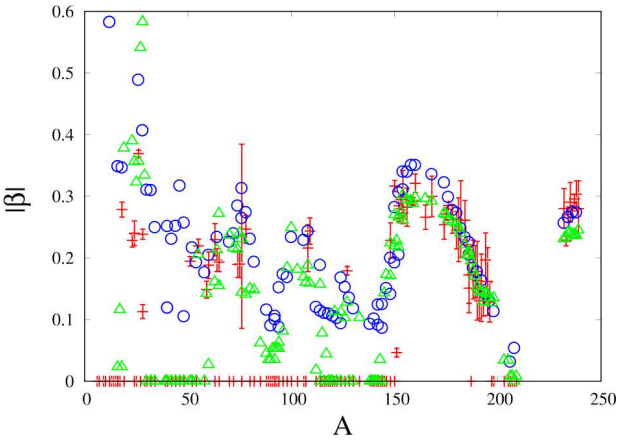


***Fig. 2.*** Absolute values of the quadrupole deformation parameter determined using the SLO model, "deflib.dat", and [9]. Symbols: crosses with error bars – SLO model (Eqs (3), (8), and (9)), triangles – database [30]; circles – database [9]

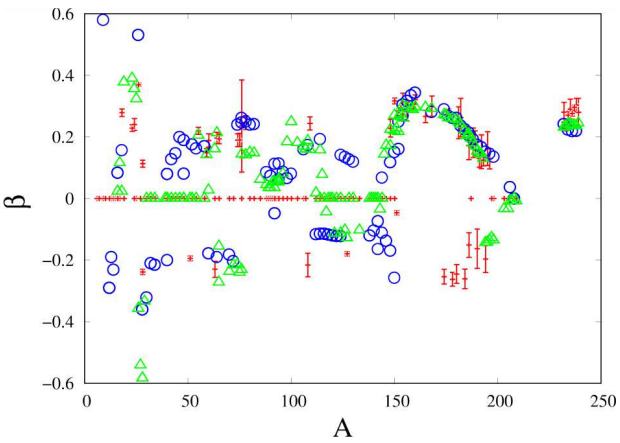


***Fig. 3.*** Comparison of the quadrupole deformation parameter values obtained from photoabsorption cross-sections using the SLO model [formulas (3), (8), and (9)] and values from the "deflib.dat" [30] and [6] databases. Symbols: crosses with error bars – SLO model (Eqs (3), (8), and (9)); triangles – database [30]; circles – database [6]

values for axially symmetric nuclei, which were calculated using both the exact expression and its approximation, coincide within the calculation error limits. The quadrupole deformation parameter values, which were obtained from the energies calculated in the SLO and SMLO methods, have very close values in almost all situations.

In Fig. 2, the absolute values of the quadrupole deformation parameter calculated using the energy values obtained in the SLO model and relationship (3) are compared with corresponding theoretical values from the file "deflib.dat" [30] and with the values from the experimental database [9], where they were obtained from the probabilities of *E2* gamma transitions between the ground state and the first excited rotational state $2^+$ in even-even nuclei. One can see that, for most nuclei, the absolute values of deformation parameter have very close values and almost coincide with the theoretical values from the file "deflib.dat". Note that, in work [19], as well as in the earlier work [11], when finding the GDR parameters, the photoabsorption cross-sections in deformed nuclei (mainly those that cannot be considered as axially symmetric) were described better by means of a single Lorentzian, and the effective quadrupole deformation parameter was equal to zero for them, $\beta \equiv \beta_{\text{eff}} = 0$. From Fig. 2, one can see that in such cases, there is no agreement between the $\beta_{\text{eff}}$-values calculated from photoabsorption data and the quadrupole deformation parameter values available in other databases.

In Fig. 3, the effective quadrupole deformation parameter values determined using the photoabsorption cross-section data, the SLO model, and formulas (3), (8), and (9) are compared with the corresponding values from the "deflib.dat" database and work [6]. One can see that the signs of the deformation parameter values calculated from the photonuclear data (the SLO model for the energy) and the signs of the corresponding values taken from other databases can be opposite. According to formulas (1)–(6), the sign of the quadrupole deformation parameter depends on the ratios between the contributions of two GDR excitation modes. When fitting the photoabsorption cross-sections, the energies of GDR excitation modes were described most accurately because the least-squares fitting was performed in an energy interval near the resonance peaks. The systematic error for the values of the GDR mode contributions, which were determined over the entire energy interval, can be very large and, therefore, is unreliable, so only the absolute values of the quadrupole deformation parameter can be determined for sure. That is, in our opinion, the discrepancy in the sign of the parameter $\beta$ value determined from photoabsorption data and the $\beta$-signs in other databases occurs due to the errors obtained while determining the ratio between the contributions of the excitation modes to the integrated photoabsorption cross-section. However, as is

indicated below, such a sign discrepancy exists when comparing the parameter values from the databases [30] and [6].

In Table, the effective quadrupole deformation parameters $\beta \equiv \beta_{\text{eff}}$ are quoted for all deformed nuclei that were obtained in the axially-symmetric-nucleus approximation from the data on photoabsorption cross-sections, where the most significant discrepancies arise. The obtained values are compared with the values from the databases [30], [6], and [9]. The dashes mean the absence of corresponding values.

For the atomic nuclei presented in the table, the deformation signs are the main source of discrepancies. These discrepancies are observed not only when comparing the values obtained from the photoabsorption data, but also the values taken from other databases. In particular, such discrepancies take place for the$^{26}$Mg, $^{60}$Ni, $^{64}$Zn, $^{74}$Ge, $^{148}$Nd, $^{150}$Nd, $^{151}$Eu, and$^{196}$Pt isotopes. In some situations, photonuclear data make it possible to estimate the quadrupole deformation parameter for isotopes that are absent from the experimental databases, e.g., $^{63}$Cu, $^{65}$Zn, $^{75}$As,$^{151}$Eu,$^{185}$Re,$^{189}$Os,$^{191}$Ir,$^{195}$Pt,$^{235}$U, and $^{239}$Pu [6,9], and confirm the results of theoretical calculations in the framework of the applied approach for values from the database [30].

In Figure 4, the reactions $^{100}\text{Mo}(\gamma, n)^{99}\text{Mo}$ and $^{178}\text{Hf}(\gamma, p)^{177}\text{Lu}$ as examples, the influence of quadrupole deformation parameter on the photonuclear reaction cross-section is considered. Such reactions were chosen, because they lead to the production of radioisotopes used in medical physics, namely, $^{177}$Lu and $^{99\text{m}}$Tc (the latter after the $\beta$-decay of the isotope $^{99}$Mo).

The cross-sections were calculated using the EMPIRE 3.2 code [39] using the GDR parameters for the cross-sections of compound nuclei, which were calculated from the systematics (see Appendix) and $\beta$-deformation values taken from various databases. In the EMPIRE code, the default GDR parameters for the $^{100}$Mo and $^{178}$Hf nuclei were replaced by new ones calculated in this work. The SLO model was used for the photon strength function. All other input parameters for the calculations remained standard by default; for example, the EGSM model of the EMPIRE code was used for the densities of nuclear levels. The experimental data were taken from the library [37], and the estimated data from the TENDL2023 library [40], where the code [41] was used for calculations.

In Fig. 4, the following notations are adopted: the solid curves demonstrate the results of calculations using the GDR characteristics from the table of work [19] for the SLO model (in particular, $\beta = 0.0$ for $^{100}$Mo, and $\beta = -0.26$ for $^{178}$Hf); the dashed curves correspond to the results of calculations with the GDR parameters calculated according to systematics (A4)–(A8) with the deformation parameter values

**Effective quadrupole deformation parameters $\boldsymbol{\beta \equiv \beta_{\text{eff}}}$ in the axially-symmetric-nucleus approximation, where the most substantial discrepancies in the values from various databases take place**

| Nucleus | $\beta$, $E_i$-SLO, (3) | $\beta$, $E_i$-SLO, (4) | $\beta$, "deflib.dat" [30] | $\beta$, [6] | $\lvert\beta\rvert$, [9] |
|---|---|---|---|---|---|
| $^{14}$C | 0.64(2) | 0.593(12) | – | –0.231 | – |
| $^{26}$Mg | 0.369(6) | 0.351(4) | –0.357 | 0.531 | 0.4891 |
| $^{28}$Si | –0.239(8) | –0.24(1) | –0.583 | –0.360 | 0.4073 |
| $^{60}$Ni | 0.19(2) | 0.18(2) | 0.027 | –0.178 | 0.2052 |
| $^{63}$Cu | –0.23(3) | –0.23(3) | 0.161 | – | – |
| $^{64}$Zn | 0.20(2) | 0.19(2) | 0.213 | –0.190 | 0.2342 |
| $^{65}$Zn | 0.19(2) | 0.187(14) | –0.272 | – | – |
| $^{74}$Ge | 0.19(2) | 0.18(2) | –0.214 | 0.240 | 0.2850 |
| $^{75}$As | 0.19(2) | 0.18(2) | –0.240 | – | – |
| $^{78}$Se | 0.25(2) | 0.24(2) | 0.141 | 0.250 | 0.2744 |
| $^{108}$Pd | –0.22(4) | –0.22(4) | 0.188 | 0.174 | 0.2437 |
| $^{148}$Nd | 0.23(3) | 0.22(2) | 0.224 | –0.169 | 0.2004 |
| $^{150}$Nd | 0.317(9) | 0.303(8) | 0.270 | –0.257 | 0.2825 |
| $^{151}$Eu | –0.046(7) | –0.046(7) | 0.228 | – | – |
| $^{156}$Gd | 0.28(3) | 0.27(3) | 0.295 | 0.317 | 0.3399 |
| $^{168}$Er | 0.30(3) | 0.29(3) | 0.292 | 0.281 | 0.3361 |
| $^{174}$Yb | –0.25(2) | –0.26(3) | 0.272 | 0.290 | 0.3226 |
| $^{178}$Hf | –0.26(2) | –0.27(3) | 0.259 | 0.262 | 0.2779 |
| $^{180}$Hf | –0.25(3) | –0.25(3) | 0.256 | 0.262 | 0.2731 |
| $^{182}$W | 0.26(6) | 0.25(5) | 0.240 | 0.237 | 0.2485 |
| $^{184}$W | –0.26(3) | –0.27(4) | 0.221 | 0.225 | 0.2339 |
| $^{186}$W | –0.15(4) | –0.15(4) | 0.210 | 0.214 | 0.2257 |
| $^{185}$Re | 0.221(13) | 0.214(12) | 0.204 | – | – |
| $^{186}$Os | 0.17(5) | 0.17(4) | 0.205 | 0.205 | 0.2056 |
| $^{188}$Os | 0.18(5) | 0.18(4) | 0.179 | 0.193 | 0.1844 |
| $^{189}$Os | 0.18(4) | 0.17(4) | 0.170 | – | – |
| $^{190}$Os | –0.16(6) | –0.16(7) | 0.153 | 0.175 | 0.1777 |
| $^{192}$Os | 0.15(5) | 0.15(5) | 0.145 | 0.167 | 0.1639 |
| $^{191}$Ir | 0.13(3) | 0.13(3) | 0.147 | – | – |
| $^{194}$Pt | –0.20(4) | –0.20(5) | –0.143 | 0.152 | 0.1421 |
| $^{195}$Pt | 0.16(5) | 0.16(5) | –0.142 | – | – |
| $^{196}$Pt | 0.13(3) | 0.13(3) | –0.135 | 0.146 | 0.1308 |
| $^{235}$U | 0.29(3) | 0.28(3) | 0.241 | – | – |
| $^{239}$Pu | 0.28(5) | 0.27(4) | 0.245 | – | – |

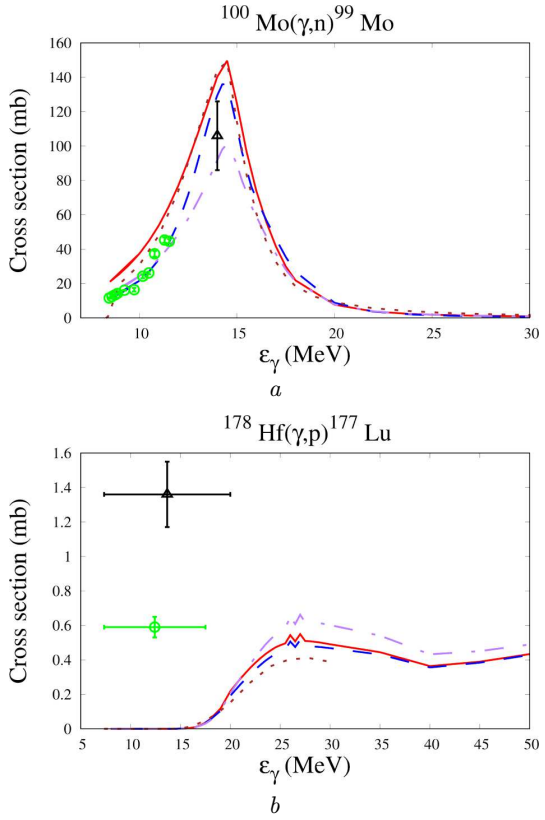


***Fig. 4.*** Dependences of the cross-sections of the nuclear reactions $^{100}$Mo$(\gamma, n)^{99}$Mo ($a$) and $^{178}$Hf$(\gamma, p)^{177}$Lu ($b$) on the gamma-ray energy. Notation: solid curves – calculations using the GDR characteristics from work [19] for the SLO model ($\beta = 0.0$ for $^{100}$Mo, and $\beta = -0.25$ for $^{178}$Hf); dashed curves – calculations with the GDR parameters calculated according to systematics (A4)–(A8) with deformation parameter values taken from database [30] ($\beta = 0.249$ for $^{100}$Mo, and $\beta = 0.256$ for $^{178}$Hf); dash-dotted curves – single-resonance approximation with the energies $E_0^{\rm SLO}$ according to formula (A4) and the widths according to formula (A8) with $\beta$-values taken from [30]; dotted curves – data from the TENDL2023 library. Experimental data: files with numbers K2373002 (triangles), K2433007 (circles) from the EXFOR library with data from works [42] and [43] ($a$); files with numbers M1020006 (triangles), M1020007 (circles) from the EXFOR library with data from work [44] ($b$)

taken from the "deflib.dat" database [30] ($\beta = 0.249$ for $^{100}$Mo, and $\beta = 0.259$ for $^{178}$Hf) and the systematic parameters of the SLO model; the dash-dotted curves illustrate the single-resonance approximation with the energy $E_0^{\rm SLO}$ calculated according to formula (A4), the width $\Gamma_0^{\rm SLO}$ according to formula (A8), and the $\beta$-values taken from the database [30]; and the dotted curves are the data from the TENDL2023 library. Except for the calculations with the GDR characteristics taken from the table in work [19], in all other cases, the contributions to the integrated photoabsorption cross-section were determined using relationship (7) with $s_\Sigma = 1.2$, where the vibration modes and the $s_a$- and $s_b$-values were according to the deformation sign.

Experimental data are depicted in Fig. 4 as follows. In Fig. 4, $a$: the files with numbers K2373002 (triangles) and K2433007 (circles) from the EXFOR library with the data from works [42] and [43]; in Fig. 4, $b$: the files with numbers M1020006 (triangles) and M1020007 (circles) from the EXFOR library with the data from work [44]. The experimental data in Fig. 4, $b$ are the cross-sections

$$\langle\sigma\rangle = \int\limits_{E_{\rm trh}}^{E_e} \sigma(\varepsilon_\gamma) w(\varepsilon_\gamma) d\varepsilon_\gamma$$

averaged over the density

$$w(\varepsilon_\gamma) = \varphi(\varepsilon_\gamma) / \int\limits_{E_{\rm trh}}^{E_e} \varphi(\varepsilon_\gamma) d\varepsilon_\gamma$$

of the bremsstrahlung intensity distribution $\varphi(\varepsilon_\gamma)$. The quantity $E_{\rm trh} = 7.34$ MeV is the energy threshold of the reaction $(\gamma, p)$,and $E_e$ is the maximum bremsstrahlung energy, which equals 17.5 MeV for the data from M1020006, and 20 MeV for the data from the file M1020007. The values of the averaged cross-section are indicated at the average energy

$$\langle\varepsilon_\gamma\rangle = \int\limits_{E_{\rm trh}}^{E_e} \varepsilon_\gamma w(\varepsilon_\gamma) d\varepsilon_\gamma,$$

and the energy uncertainty of gamma-rays corresponds to the spread interval of the bremsstrahlung energy $\varepsilon_\gamma \in [E_{\rm trh}, E_e]$.

The general behavior of the cross-sections for all calculation results is identical, and the cross-sections have a single-resonance appearance irrespective of whether the nucleus is considered to be spherical or axially symmetric. Two GDR modes do not manifest themselves owing to their rather large width. For the $^{178}$Hf nucleus, although the deformation signs taken while calculating using the SLO model and the "deflib.dat" database were opposite, this fact did not significantly affect the single-resonance behavior of the

cross-sections. At the same time, the application of different values and signs of the deformation parameter can change the cross-section value at its maximum by up to 40%. For the $^{100}$Mo nucleus, the best agreement with experiment was obtained when calculating in the axially-symmetric-nucleus approximation with the deformation taken from the database [30]. For the $^{178}$Hf nucleus, the values of all calculated cross-sections differ substantially from their average experimental values.

## 3. Conclusions

From the values of the GDR energy splitting in the photoabsorption cross-sections, the values of the effective quadrupole deformation parameter of atomic nuclei are obtained, and their uncertainties are estimated. The values of the energies and contributions of the GDR modes are taken from the tables in works [19, 21] for 144 isotopes of atomic nuclei from $^{6}$Li to $^{239}$Pu. To calculate the deformation parameter in the axially-symmetric-nucleus approximation, relationship (3) and its approximation (4), (7) are used in accordance with the generalized hydrodynamic model of Danos [22]. In the rare-earth ($155 < A < 190$) and actinide ($225 < A < 250$) intervals, the obtained $\beta$-values are the values of the quadrupole shape deformation parameter, whereas for other nuclei, the obtained values correspond to the effective nucleus deformation parameter $\beta \equiv \beta_{\text{eff}}$, when the nucleus shape is approximated by an ellipsoid of rotation. The approximate expressions (4) and (7) make it possible to calculate the absolute values of the quadrupole deformation parameter without determining the type of vibration mode, namely, whether it refers to vibrations along or perpendicular to the nucleus symmetry axis.

The calculations are carried out with the GDR characteristics obtained in the SLO and SMLO approaches to describe the photon strength functions. The results were compared with the values obtained in other approaches [6, 8, 9], and also with the database in the file "deflib.dat"[30], where they were calculated using the macro-microscopic approach [31].

The signs of the deformation parameter, which were determined from the photonuclear data (the SLO model for energies) and from the libraries "deflib.dat"[30] and [6] can be opposite. This is due to the fact that the sign of the quadrupole deformation parameter depends on the ratio between the contributions of two GDR excitation modes, which are determined with a large error. The energies of the GDR excitation modes are described most accurately, because the least-squares fitting was performed in the energy interval near the resonance peaks. Note, however, that the discrepancies in the signs of $\beta$ parameter took place not only when comparing the values obtained from the photoabsorption data, but also the values taken from other databases.

It is demonstrated that, in most situations, the values obtained for the absolute value of the quadrupole deformation parameter at the GDR excitation coincide within the error limits, with the equilibrium absolute values of the quadrupole deformation parameter in the ground states of axially symmetric nuclei. That is, the considered method for determining the absolute values of the $\beta$ parameter can be considered to be a sufficiently reliable alternative method for determining the absolute values of the quadrupole deformation parameter.

For the $^{100}$Mo and $^{178}$Hf nuclei, photoabsorption cross-sections with various values of GDR characteristics are calculated. The general behavior of the cross-sections for all calculation results is identical, and the cross-sections have a single-resonance appearance regardless of whether the nucleus is considered to be spherical or axially symmetric. Despite the presence of a deformation, two GDR modes do not manifest themselves because of their rather large width. However, taking the nucleus deformability into account has a rather considerable effect on the cross-section values in a vicinity of the resonance. The application of various values and signs of the deformation parameter can change the cross-section value at its maximum by up to 40%.

*The authors thank the NFDU Foundation for partial support of their research (NFDU grant 2023.05/0024 "Addressing contemporary issues in chemistry, biomedicine, physics, and materials science using high-performance computing and machine learning").*

### APPENDIX.
### Calculation of the Cross-Section of the Compound Nucleus Formation by Gamma Quanta and the Systematics of GDR Parameters

As the cross-section $\sigma_{\text{CN}}$ of the compound nucleus formation by gamma quanta of the dipole electric type ($E1$), the averaged photoabsorption cross-section of such radiation is used. For

gamma rays with energies $\varepsilon_\gamma \leq 50$ MeV, this cross-section can be considered to equal the average total cross-section $\sigma_{\rm gdr}$ of photoabsorption due to GDR excitation. The latter can be calculated using the $E1$ photon strength functions (PSFs) of photoabsorption $\mathbf{f}^\alpha_{E1}(\varepsilon_\gamma)$,

$$\sigma^\alpha_{\rm CN}(\varepsilon_\gamma) = \sigma^\alpha_{\rm gdr}(\varepsilon_\gamma) = 3\,(\pi\hbar c)^2\,\varepsilon_\gamma \mathbf{f}^\alpha_{E1}(\varepsilon_\gamma), \tag{A1}$$

where the superscript $\alpha$ denotes the PSF model used in the calculations (in this work, $\alpha =$SLO, SMLO [14, 17, 20, 34–36, 38]).

The PSF is determined via the spectral function $\Phi_{\rm gdr}\,(\varepsilon_\gamma, T)$ whose general expression in the case where gamma quanta of type $E1$ are absorbed by a nucleus heated to the temperature $T$ with the GDR excitation looks like

$$\begin{aligned}
&\mathbf{f}^\alpha_{E1}(\varepsilon_\gamma) = \Phi^\alpha_{\rm gdr}(\varepsilon_\gamma, T) = \\
&= \frac{1}{3(\pi\hbar c)^2}\sum_{j=1}^{j_m}\sigma_{\rm TRK}\, s^\alpha_j \frac{\bar F^\alpha_j(\varepsilon_\gamma, T)}{\varepsilon_\gamma} = \\
&= 8.674\times 10^{-8}\sum_{j=1}^{j_m}\sigma_{\rm TRK}\,[\text{mb}\cdot\text{MeV}]\times \\
&\times s^\alpha_j \frac{\bar F^\alpha_j(\varepsilon_\gamma, T)\,[\text{MeV}^{-1}]}{\varepsilon_\gamma\,[\text{MeV}]}.
\end{aligned} \tag{A2}$$

Here, the subscript $j$ denotes the number of normal GDR excitation modes; and $j_m = 1$ for a spherical nucleus, and $j_m = 2$ for an axially symmetric one. The multiplier $\sigma_{\rm TRK}$ is the value of the Thomas–Reich–Kuhn (TRK) sum rule: $\sigma_{\rm TRK} = 60NZ/A = 15A(1-I^2)$ [mb$\cdot$MeB] with $I = (N-Z)/A$. The function $\bar F^\alpha_j(\varepsilon_\gamma, T)$ describing the GDR excitation line shape was taken in the form of the generalized Lorentz curve,

$$\bar F^\alpha_j(\varepsilon_\gamma, T) = \frac{2}{\pi}\frac{\varepsilon^2_\gamma\,\Gamma^\alpha_j(\varepsilon_\gamma, T)}{\left[\varepsilon^2_\gamma - (E^\alpha_j)^2\right]^2 + \left[\Gamma^\alpha_j(\varepsilon_\gamma, T)\varepsilon_\gamma\right]^2}, \tag{A3}$$

where $E^\alpha_j$ ($E^\alpha_2 \geq E^\alpha_1$) and $\Gamma^\alpha_j$ are the energy and width, respectively, of the $j$-th GDR excitation mode; and $s^\alpha_j$ is the contribution (strength) of the $j$-th vibration mode. For the standard Lorentzian model ($\alpha =$SLO), the width $\Gamma^{\rm SLO}_j$ is a constant equal to the GDR width, and the energy $E^{\rm SLO}_{r,j}$ is equal to the GDR energy for the $j$-mode, and $s^{\rm SLO}_j = \sigma^{\rm SLO}_j\cdot\Gamma^{\rm SLO}_j/\sigma_{\rm TRK}$ with the value $\sigma^{\rm SLO}_j$ for the photoabsorption cross-section of the $j$ mode at the resonance energy.

In the simplified modified Lorentzian model ($\alpha =$ SMLO), the width is considered to be a linear function of the energy of gamma quanta: $\Gamma^{\rm SMLO}_j(\varepsilon_\gamma) = \varepsilon_\gamma\cdot\Gamma^{\rm SMLO}_j/E^{\rm SMLO}_{r,j}$. The values of the GDR widths for the SLO and SMLO models were also taken either from the tables of works [19, 21] or according to the systematics.

The systematics of the GDR characteristics were obtained by fitting experimental photoabsorption cross-sections using Lorentzian curves in works [19, 36, 38]. The systematics for the resonance energies was obtained from the least-squares fitting of the recommended experimental GDR parameters simultaneously in the spherical and axially symmetric nuclei ($150 < A < 190$ and $220 < A < 253$). It has the following form (in MeV units):

$$E^\alpha_0 = e^\alpha_1 A^{-1/3}\sqrt{\frac{1-I^2}{1+e^\alpha_2 A^{-1/3}}}, \tag{A4}$$

where the coefficients $e^\alpha_1$ and $e^\alpha_2$ are as follows: for the SLO model, $e^{\rm SLO}_1 = 130.0(9)$ and $e^{\rm SLO}_2 = 9.0(2)$; for the SMLO model, $e^{\rm SMLO}_1 = 128.0(9)$ and $e^{\rm SMLO}_2 = 8.5(2)$. The $E^{\rm SLO}_j$-value corresponds to the GDR resonance energy in spherical nuclei ($E^{\rm SLO}_j \equiv E^{\rm SLO}_0$) and the average resonance energy in axially symmetric nuclei defined as [10, 19, 36, 38]

$$E^\alpha_0 = \frac{1}{s_\Sigma}(s^\alpha_1\,E^\alpha_1 + s^\alpha_2\,E^\alpha_2), \tag{A5}$$

where $E^\alpha_1$ and $E^\alpha_2$ are the energies of the GDR modes with smaller and larger values, and $s^\alpha_1$ and $s^\alpha_2$ are their respective strengths. The correspondence of the resonance parameters – in particular, the energies – to the parameters of vibration modes along, $E^\alpha_a$, and perpendicular, $E^\alpha_b$, to the symmetry axis in axial nuclei depends on the sign of the quadrupole deformation parameter:

$$\begin{aligned}
&\beta > 0 => E_1 = E_a, E_2 = E_b,\\
&s_1 = s_a, s_2 = s_b = 2s_a,\\
&\Gamma_1 = \Gamma_a, \Gamma_2 = \Gamma_b,\\
&\beta < 0 => E_1 = E_b, E_2 = E_a,\\
&s_1 = s_b, s_2 = s_a = s_b/2,\\
&\Gamma_1 = \Gamma_b, \Gamma_2 = \Gamma_a.
\end{aligned} \tag{A6}$$

For calculating the energies, the following approximations were adopted:

$$\begin{aligned}
E_a &= E_0\cdot\frac{R'_0}{R_a} = \frac{E_0}{1+0{,}631\beta},\\
E_b &= E_0\cdot\frac{R'_0}{R_b} = \frac{E_0}{1-0{,}631\beta/2}.
\end{aligned} \tag{A7}$$

For the systematics of the resonance width, the power-law expression was adopted,

$$\Gamma^\alpha_j = c^\alpha (E^\alpha_j)^{d^\alpha}\ [\text{MeV}], \tag{A8}$$

with the following fitting parameters of the experimental GDR widths: $c^{\rm SLO} = 0.32(3)$, $d^{\rm SLO} = 0.98(3)$ and $c^{\rm SMLO} = 0.42(5)$, $d^{\rm SMLO} = 0.90(4)$.

Note that for axially deformed nuclei, the spherical-nucleus approximation is often used, and the photoabsorption cross-section is approximated by expressions with one Lorentzian, i.e., formulas (A1) and (A2) with $j = 1$ are used. If there are no GDR characteristics from fitting the photoabsorption experimental data, systematics (A4) is used as the resonance energy. The width of the resonance curve is calculated by the formula [23, 28]

$$\Gamma^\alpha_0 = |E^\alpha_1 - E^\alpha_2| + \frac{\Gamma^\alpha_1}{2} + \frac{\Gamma^\alpha_2}{2}\ [\text{MeV}], \tag{A9}$$

where relationships (A6)–(A8) with the deformation values taken from the file "deflib.dat" are used for the energies and widths in the $j$-th resonance mode. Note that the approximation of the photoabsorption cross-sections of axially symmetric nuclei by a single Lorentzian with width (A9) corresponds to a situation when the distance between the peaks is considerably smaller than the half-width sum of the peaks.


1. A. Bohr, B. R. Mottelson. *Nuclear Structure. Vol. II. Nuclear Deformation* (Addison-Wesley, 1998), Ch. 4.
2. O. Nathan, S.G. Nilsson. Collective nuclear motion and the unified model. In: *Alpha-, Beta- and Gamma-Ray Spectroscopy. Vol. II.* Edited by K. Siegbahn (North-Holland, 1965).
3. K.E. Lobner, M. Vetter, V. Honig. Nuclear intrinsic quadrupole moments and deformaion parameters. *Nucl. Data Tabl.* **7**, 495 (1970).
4. P. Raghavan. Table of nuclear moments. *At. Data Nucl. Data Tabl.* **42**, 189 (1989).
5. N.J. Stone. Table of nuclear magnetic dipole and electric quadrupole moments. *At. Data Nucl. Data Tabl.* **90**, 75 (2005).
6. A.V. Yushkov. Surface of $b(Z, N)$ deformation for nuclei with $Z$ from 2 to 102. *Phys., Elem. Part. At. Nucl.* **24**, 348 (1993).
7. S. Raman, C.H. Malarkey, W.T. Milner, C.W. Nestor Jr., P.H. Stelson. Transsition probability, B(E2)up, from the ground to first excited $2^+$ state of even-even nuclides. *At. Data Nucl. Data Tabl.* **36**, 1 (1987).
8. S. Raman, C.W. Nestor Jr., P. Tikkanen. Transition probability from the ground to the first-excited $2^+$ state of even-even nuclides. *At. Data Nucl. Data Tabl.* **78**, 1 (1987).
9. B. Pritychenko, M. Birch, B. Singh, M. Horoi. Tables of E2 transition probabilities from the first $2^+$ states in even–even nuclei. *At. Data Nucl. Data Tabl.* **107**, 1 (2016).
10. B.L. Berman, S.C. Fultz, Measurements of the giant dipole resonance with monoenergetic photons. *Rev. Mod. Phys.* **47**, 713 (1975).
11. S.S. Dietrich, B.L. Berman. Atlas of photoneutron cross sections obtained with monoenergetic photons. *At. Data Nucl. Data Tabl.* **38**, 199 (1988).
12. A. Van der Woude. The electric giant resonances. In: *Electric and Magnetic Giant Resonances in Nuclei.* Edited by J. Speth (World Scientific, 1991), p. 99.
13. M.B. Chadwick, P. Obložinský, A.I. Blokhin, T. Fukahori, Y. Han, Y.-O. Lee, M.N. Martins, S.F. Mughabghab, V.V. Varlamov, B. Yu, J. Zhang. *Handbook on Photonuclear Data for Applications. Cross-Sections and Spectra. Tech. Rep. IAEATECDOC-1178* (International Atomic Energy Agency, 2000).
14. T. Belgya, O. Bersillon, R. Capote Noy, T. Fukahori, Ge Zhigang, S. Goriely, M. Herman, A.V. Ignatyuk, S. Kailas, A.J. Koning, P. Obložinský, V. Plujko, P.G. Young. *Handbook for Calculations of Nuclear Reaction Data. Reference Input Parameter Library-2. Tech. Rep. IAEA-TECDOC-1506* (International Atomic Energy Agency, 2006).
15. V.M. Mazur. Giant nuclear dipole resonance. *Visn. Uzhhorod Univ. Ser. Fiz.* N 13, 100 (2003) (in Ukrainian).
16. V.M. Mazur, L.M. Mel'nikova. Giant dipole resonance in absorbtion and emission of gamma rays by medium and heavy nuclei. *Phys. Part. Nucl.* **37**, 923 (2006).
17. R. Capote, M. Herman, P. Obložinský, P.G. Young, S. Goriely, T. Belgya, A.V. Ignatyuk, A.J. Koning, S. Hilaire, V.A. Plujko, M. Avrigeanu, O. Bersillon, M.B. Chadwick, T. Fukahori, Zhigang Ge, Yinlu Han, S. Kailas, J. Kopecky, V.M. Maslov, G. Reffo, M. Sin, E.Sh. Soukhovitskii, P. Talou. Reference Input Library (RIPL). *Nucl. Data Sheets* **110**, 3107 (2009).
18. V.A. Plujko, R. Capote, O.M. Gorbachenko. Giant dipole resonance parameters with uncertainties from photonuclear cross sections. *Atom. Data Nucl. Data Tables* **97**, 567 (2011).
19. V.A. Plujko, O.M. Gorbachenko, R. Capote, P. Dimitriou. Giant dipole resonance parameters of ground-state photoabsorption: Experimental values with uncertainties. *Atom. Data Nucl. Data Tables* **123–124**, 1 (2018).
20. S. Goriely, P. Dimitriou, M. Wiedeking, T. Belgya, R. Firestone, J. Kopecky, M. Krticka, V. Plujko, R. Schwengner, S. Siem, H. Utsunomiya, S. Hilaire, S. Peru, Y.S. Cho, D.M. Filipescu, N. Iwamoto, T. Kawano, V. Varlamov, R. Xu. Reference database for photon strength functions. *Eur. Phys. J. A* **55**, 172 (2019).
21. T. Kawano., Y.S. Cho, P. Dimitriou., D. Filipescu, N. Iwamoto, V. Plujko, X. Tao, H. Utsunomiya, V. Varlamov, R. Xu, R. Capote, I. Gheorghe, O. Gorbachenko, Y.L. Jin, T. Renstrøm, M. Sin, K. Stopani, Y. Tian, G.M. Tveten, J.M. Wang, T. Belgya, R. Firestone, S. Goriely, J. Kopecky., M. Krtička, R. Schwengner, S. Siem, M. Wiedeking. IAEA Photonuclear Data Library 2019. *Nucl. Data Sheet* **163**, 109 (2020).
22. M. Danos. On the long-range correlation model of the photonuclear effect. *Nucl. Phys.* **5**, 23 (1958).
23. K. Okamoto. Intrinsic quadrupole moment and the resonance width of photonuclear reactions. *Phys. Rev.* **110** (1), 143 (1958).
24. J.M. Eisenberg, W. Greiner. *Nuclear Theory. Vol. 1. Nuclear Models, Collective and Single-Particle Phenomena* (North-Holland, 1970).
25. W.D. Myers, W.J. Swiatecki, T. Kodama, L.J. El-Jaick, E.R. Hilf. Droplet model of the giant dipole resonance. *Phys. Rev. C* **15**, 2032 (1977).
26. E. Lipparini, S. Stringari. Some rules and giant resonances in nuclei. *Phys. Rep.* **175**, 103 (1989)
27. V.Yu. Denisov. Dipole resonances in the gas-droplet model of the nucleus. *Sov. J. Nucl. Phys.* **43**, 28 (1986).
28. V.Yu. Denisov. Isoscalar and isovector giant resonances in the gas-droplet model for deformed nuclei. *Sov. J. Nucl. Phys.* **44**, 20 (1986).
29. V.Yu. Denisov, V.A. Plujko. *The Problems of Physics of Atomic Nuclei and Nuclear Reactions* (Taras Shevchenko Nat. Univ., 2013) [in Ukrainian].

30. File “deflib.dat” from Section “GAMMA” project RIPL [14].
31. P. Moller, J.R. Nix, W.D. Myers, W.J. Swiatecki. Nuclear ground-state masses and deformations. *Atom. Data Nucl. Data Tabl.* **59**, 185 (1995).
32. I.M. Kadenko, V.A. Plujko. *Elements Of Estimation Methods Of Statistical Data And Their Distribution Function* (Taras Shevchenko Nat. Univ., 2003) [in Ukrainian].
33. M.B. Chadwick, P. Obložinský, P.E. Hodgson, G. Reffo. Pauli-blocking in the quasideuteron model of photoabsorption. *Phys. Rev. C* **44**, 814 (1991).
34. D.M. Brink. *Some Aspects Of Interaction Of Fields With Matter. Ph.D. thesis* (Oxford University, 1955).
35. S. Goriely, V. Plujko. Simple empirical E1 and M1 strength functions for practical applications. *Phys. Rev. C* **99**, 014303 (2019).
36. V. Plujko, O. Gorbachenko, K. Solodovnyk. Description of nuclear photoexcitation by Lorentzian expressions for electric dipole photon strength function. *Eur. Phys. J. A* **55**, 210 (2019).
37. *Experimental Nuclear Reaction Data Library EXFOR*, https://www-nds.iaea.org/exfor/.
38. V.A. Plujko, S. Goriely, O.M. Gorbachenko, K.M. Solodovnyk. Test of models for photon strength functions of electric dipole photoexcitation. *Nucl. Phys. At. Ener.* **20**, 213 (2019).
39. M. Herman, R. Capote, B.V. Carlson, P. Obložinský, M. Sin, A. Trkov, H. Wienke, V. Zerkin. EMPIRE: Nuclear reaction model code system for data evaluation. *Nucl. Data Sheets* **108**, 2655 (2007).
40. *TENDL2023 library*; https://tendl.web.psi.ch/tendl_2023/tendl2023.html.
41. A.J. Koning, S. Hilaire, M.C. Duijvestijn. TALYS: comprehensive nuclear reaction modeling. In *Proceedings of the International Conference on Nuclear Data for Science and Technology-ND 2004*. Edited by R.C. Haight, M.B. Chadwick, T. Kawano, P. Talou (AIP, 2005), p. 1154.
42. H. Ejiri, T. Shima, S. Miyamoto, K. Horikawa, Y. Kitagawa, Y. Asano, S. Date, Y. Ohashi. Resonant photonuclear reactions for isotope transmutation. *J. Phys. Soc. Jap.* **80**, 094202 (2011).
43. H. Utsunomiya, S. Goriely, T. Kondo, C. Iwamoto, H. Akimune, T. Yamagata, H. Toyokawa, H. Harada, F. Kitatani, Y.W. Lui, A.C. Larsen, M. Guttormsen, P.E. Koehler, S. Hilaire, S. Peru, M. Martini, A.J. Koning. Photoneutron cross sections for Mo isotopes: A step towards a unified understanding of $(\gamma, n)$ and $(n, \gamma)$ reactions. *Phys. Rev. C* **88** 15805 (2013).
44. V.A. Zheltonozhsky, M.V. Zheltonozhskaya, A.M. Savrasov, S.S. Belyshev, A.P. Chernyaev, V.N. Yatsenko. Studying the activation of $^{177}$Lu in $(\gamma, pxn)$ reactions. *Bull. Rus. Acad. Sci. Phys.* **84**, 923 (2020).

Received 18.02.25

*О.М. Горбаченко, В.А. Плюйко*

ПАРАМЕТРИ ДЕФОРМАЦІЇ АТОМНИХ ЯДЕР З ДАНИХ ПО ФОТОПОГЛИНАННЮ ТА ЇХ ВПЛИВ НА ПЕРЕРІЗИ ФОТОПОГЛИНАННЯ

Обчислено параметри ефективної квадрупольної деформації атомних ядер і оцінено їх невизначеності. Використано наближення аксіально-симетричних ядер і величину розщеплення енергій двох мод ізовекторного гігантського дипольного резонансу (ГДР) в перерізах фотопоглинання 144 ізотопів від $^{6}$Li до $^{239}$Pu. Для аксіально-симетричних ядер (з $155 < A < 190$ і $225 < A < 250$) визначені ефективні параметри квадрупольної деформації точно відповідають значенням параметрів квадрупольної деформації $\beta$. Результати порівнюються із отриманими в інших підходах відповідними величинами. Продемонстровано, що знайдені абсолютні значення квадрупольних параметрів деформацій при збудженні ГДР, як правило, в межах похибок збігаються із абсолютними значеннями деформацій в основному стані ядер. Для ядер $^{100}$Mo та $^{178}$Hf обчислено та проаналізовано залежності парціальних перерізів фотопоглинання від характеристик ГДР.

*Ключові слова*: перерізи фотопоглинання, аксіально-деформовані ядра, параметри квадрупольної деформації ядер, ізовекторний гігантський дипольний резонанс, розщеплення енергії.